Macromolecules
ARTICLE

Macromolecules **2010**, *43*, 4401–4411 **4401**
DOI: 10.1021/ma902769s

Rheology and Structure of Entangled Telechelic Linear and Star Polyisoprene Melts

E. van Ruymbeke,*,†,‡ D. Vlassopoulos,†,§ M. Mierzwa,∥,⊥ T. Pakula,⊥ D. Charalabidis,# M. Pitsikalis,# and N. Hadjichristidis#

†*FORTH, Institute of Electronic Structure & Laser, Heraklion, Crete, Greece,* ‡*Unité de Physique et Chimie des Hauts Polymères, Université catholique de Louvain, Louvain-la-Neuve, Belgium,* §*University of Crete, Department of Materials Science & Technology, Heraklion, Crete, Greece,* ∥*Silesian University, A.Chelkowski Institute of Physics, Katowice, Poland,* ⊥*Max-Planck Institut für Polymerforschung, Mainz, Germany, and* #*University of Athens, Department of Chemistry, Athens, Greece*

Received December 16, 2009; Revised Manuscript Received March 16, 2010

ABSTRACT: We investigate the linear viscoelastic response of model telechelic linear and star (of varying functionality) polyisoprene melts with different molar masses above the entanglement limit in relation to their structure. We find that these systems self-assemble as a result of the strong dipolar interactions and form clusters that seem to depend primarily on the number of dipolar groups per star. The dynamics is rather complex, but some pertinent features are observed: the segmental dynamics is affected by the telechelic functionalization, especially for short arm lengths; this reflects the change of microstructure (and thus glass-transition temperature) with functionalization. The terminal relaxation is much slower compared to similar nonionic stars, reflecting the relaxation of clusters. Linear semitelechelic polymers (with only one end functionalized) aggregate in a star-like fashion. We further develop a tube model based on the time-marching algorithm for stars and linear chains, where we incorporate the association status of the chains via the dipolar interactions at each time step. The agreement of the predictions with the data, using two adjustable parameters (the average times when two dipolar pair remain associated or free, respectively), is remarkable and suggests design criteria for forming desired supramolecular assemblies.

I. Introduction

Introduced in 1960,[1] telechelics are defined as polymeric molecules with reactive terminal groups that have the capacity to form intramolecular as well as intermolecular bonds. In the last 20 years, they have received a great deal of attention because of their various applications and intriguing properties. Telechelic groups can be used as a precursor of chain extension of graft polymers.[2] They can create transient networks able to flow at very long times, depending on the lifetime of the supramolecular associations. Because of the presence of different molecular interactions, such as enthalpic (hydrophobic, hydrophilic), van der Waals, and Coulombic, telechelic materials can give rise to many different self-organizing structures and conformations with a large variety of macroscopic properties.[2−35] In particular, these materials are promising for biological or medical applications[3,4,6−11] or for the development of new devices in advanced technology industries.[5]

To design new soft materials composed of supramolecular aggregates, a rigorous understanding of the role of different interactions on the self-assembling process is needed. Different theoretical and simulation works have been proposed in this direction[13−27] for both melts and solutions of self-assembling functionalized polymers. In particular, understanding the dynamics of self-associating polymers carrying one or more associating terminal groups has attracted strong interest, supported by the considerable progress achieved in synthesizing polymers with well-defined number and positions of the specific reactive groups.[2,28−39] Telechelic polymers are characterized by a very long time dependence of the network structure[29,40−42] and an ability to create clusters.[35,43−46] Among them, model macromolecules with polar end groups represent a simple system to study the mechanism driving intra- and intermolecular aggregation and related properties.[2,24,40−42,47−54] Such polymers of different architectures were obtained from anionic synthesis.[35,40,52−54]

In previous work, we have shown that selective functionalization of linear and three-arm star polymers (of varying molecular weights) with strong dipolar end groups yields a variety of self-organized structures and a respective dynamics much different from that of the nonfunctionalized precursor polymers, thus providing a means for supramolecular structural control.[47,48,55] Despite the progress in understanding supramolecular systems, the melt dynamics of highly entangled telechelic stars of varying functionalities and molecular weights has not been addressed. Here we take-up on this challenge and present a complete analysis that, we believe, is applicable to different architectures. On the basis of previous works on nonionic branched polymers,[55,56] we propose a tube-based model able to account for both the associating dynamic of telechelic groups and the molecular entanglements. By comparing theoretical and experimental results, we obtain a deeper understanding of the linear viscoelastic response of these telechelic samples. We address the effect of arm functionality on the properties of telechelic stars with all arms capped with the dipolar groups. We also discuss the differences in behavior between linear and star telechelic polymers. Our findings suggest general design guidelines for obtaining soft supramolecular structures with tunable properties.

The remainder of this article is divided in different sections as follows: Section II presents the experimental details and Section III presents the modeling approach used. Results are

*Corresponding author. E-mail: evelyne.vanruymbeke@uclouvain.be.

Published on Web 04/09/2010

presented and discussed in Section IV. Finally, the main conclusions are summarized in the last section.

II. Experimental Section

II.1. Materials. The synthesis and characterization of the ω-functionalized linear and star (with 3 and 12 arms) polyisoprenes used in this work is described in detail elsewhere.[53] Here we briefly outline the essential elements of the synthetic procedure yielding nearly monodisperse well-defined telechelic polymers. We employed anionic polymerization high-vacuum techniques and chlorosilane chemistry. 3-Dimethylaminopropyllithium (DMAPLi) was used as a functional initiator to introduce dimethylamine end groups in the polymeric chain. The 3- and 12-arm stars were prepared by coupling a small excess of the linear living chains with trichloromethylsilane and tetra[2(trichlorosilyl)ethyl]silane, respectively. The linking reaction was allowed to take place for 3 to 4 weeks. The excess arms were removed by fractionation in a toluene/methanol mixture as a solvent/nonsolvent system. The incorporation of the zwitterionic group was accomplished by the reaction of the amine-capped polymers with 2-ethoxy-2-oxo-1,3,2-dioxaphospholane, synthesized from ethanol and 2-chloro-2-oxo-1,3,2-dioxaphospholane. The reaction was allowed to proceed for 5 days under an inert atmosphere at room temperature. ^{1}H NMR analysis showed that the incorporation of the end group was quantitative.

The linear samples with one phosphoro-zwitterionic end group are called thereafter semitelechelic polyisoprenes and coded as PZw-PI, whereas the telechelic linear samples with two end groups are coded as 2PZw-PI, the 3-arm telechelic stars are coded as 3PZw-PI, and the 12-arm stars as 12PZw-PI. (See Figure 1.) With the exception of the telechelic linear sample, from each group of the telechelic polyisoprenes, three different molecular weights were employed, differing roughly by a factor of two from each other. The molecular characteristics of all samples are listed in Table 1.

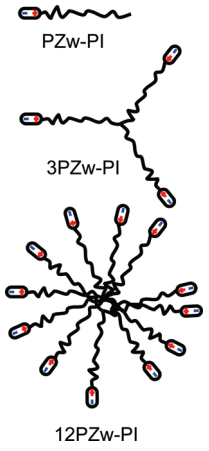

Figure 1. Cartoon representations of the linear semitelechelic and star (with 3 and 12 arms) telechelic phosphoro-zwitterionic polymers used.

II.2. Methods. *SAXS.* Measurements were conducted using a rotating anode (Rigaku 18 kW) X-ray beam with a pinhole collimation and a 2D detector (Bruker) with 1024 × 1024 pixels. A double graphite monochromator for the Cu Kα radiation (λ = 0.154 nm) was used. The beam diameter was ~0.5 mm, and the sample-to-detector distance was 1.3 m. Measurements were performed at room temperature for films of ~1 mm thickness. The recorded 2D scattered intensity distributions were averaged over the azimuthal angle and are presented as functions of the scattering vector ($s = 2 \sin\theta/\lambda$, where 2θ is the scattering angle).

Rheology. Dynamic mechanical measurements were performed by means of the Rheometrics (now TA) RMS 800 mechanical spectrometer. Shear deformation was applied under conditions of controlled deformation amplitude, always remaining in the range of linear viscoelastic response. Frequency dependencies of the storage (G') and loss (G'') shear moduli were measured in the frequency range 0.1−100 rad/s at a deformation amplitude ranging from 0.5 to 20% depending on temperature and at various temperatures between 223 and 343 K. The extracted data were shifted along the frequency axis by means of time−temperature superposition (tTS), yielding a master curve. The geometry of parallel plates was employed with plate diameters of 6 mm and a sample thickness of ~1 mm. Temperature control (±0.1 °C) was achieved via liquid and gas nitrogen. Before measurements, the samples were annealed for 48 h in vacuum at 60 °C, whereas at each temperature, the equilibration was checked with dynamic time sweep measurements (over the course of up to 3 h). The thermal expansion of the plates and change of material density with temperature were taken into account.

Dielectric Spectroscopy. The setup for the dielectric measurements consisted of the temperature-controlled sample cell and a Novocontrol system including an Alpha frequency response analyzer and a Quattro temperature controller. The samples were sandwiched between two copper electrodes of diameter 20 mm with a thickness of ~50 μm. Teflon spacers were used to control the sample geometry. The dielectric measurements were carried out at different temperatures in the range from 153 to 373 K and frequencies in the range from 10^{-2} to 10^6 Hz. The complex dielectric permittivity $\varepsilon^* = \varepsilon' - i\varepsilon''$, where ε' is the real and ε'' is the imaginary part, was recorded as a function of frequency, ω, and temperature, T.

III. Modeling Considerations

For describing the relaxation of associating polymers, both the entanglement dynamics and the association process must be taken into account to predict the relaxation of well-entangled polymers correctly. Associating polymers will relax in the same way as their corresponding nonfunctionalized chains, that is, by

Table 1. Molecular Characteristics of the Telechelic Polyisoprene Samples Used

sample code	f^a	M_a [g/mol]^b	$(M_w/M_n)_{arm}{}^c$	$(M_w)_{total}$ [g/mol]^d	$(M_w/M_n)_{star}$	T_g [°C]^e
PZw-PI-20	(2)	19 600	1.06	20 900	1.06	−56.0
PZw-PI-45	(2)	47 300	1.05	55 300	1.05	−57.4
PZw-PI-100	(2)	104 800	1.03	110 100	1.03	−60^f
2PZw-PI-10	(2)	10 000	1.09	23 200	1.32	−50.1^f
3PZw-PI-5	3	5100	1.09	17 000	1.10	−40^f
3PZw-PI-10	3	10 000	1.09	33 700	1.06	−50.1^f
3PZw-PI-20	3	20 000	1.05	66 500	1.05	−51.2
12PZw-PI-10	12	10 000	1.09	110 000	1.06	−50.1
12PZw-PI-20	12	20 000	1.05	245 000	1.05	−55.5
12PZw-PI-45	12	41 700	1.06	520 000	1.06	−57.4

[a] Number of arms (functionality). Linear chains are sometimes considered as the limit where f = 2, but this is of no relevance for the present semitelechelic linear polymers. [b] Number-average arm molar mass. In the case of linear chains, the reported value is the total molecular weight. For the linear polyisoprenes, this number refers to the total molar mass. [c] Polydispersity in arm molar mass. [d] Total linear or star weight-average molar mass. [e] Determined as the middle point of the enthalpy step in the DSC second heating trace. [f] Estimated on the basis of refs 53 (for determining the microstructure) and 71 (for determining the dependence of T_g on microstructure for polyisoprenes).

reptation, contour length fluctuations (CLFs), and by constraint release mechanism (CR).[56] However, an important difference is that a telechelic branch can relax only if its chain end is not associated. We have taken into account this possibility and appropriately extended the time-marching algorithm (TMA) for entangled nonionic polymers[56] by assessing the associating status of each molecule at each time step. This allows updating (if the chain end is not associated) or not (if the chain end is associated) the survival probabilities of each molecular segment (by reptation or CLF). To simplify the modeling, one important assumption is made, which is usually valid for telechelic polymers (and in particular, for the samples analyzed in this work): we consider that the average time during which a telechelic branch remains associated, $\tau_{associated}$, is very long, much longer than the average lifetime, during which it will stay unassociated, τ_{free}, and much longer than the fluctuations times, $\tau_{fluc}(x)$, of the different molecular segments of a unassociated branch: $\tau_{associated} \gg \tau_{free}, \tau_{fluc}(x)$.

Also note that for well-entangled telechelic polymers, the relaxation times of a branch that is dissociated and therefore able to relax can be quite long, as observed with classical covalent star polymers. Therefore, it is expected that such a well-entangled chain will not be able to fully relax (e.g., by CLFs) before associating again with other telechelic junctions (i.e., $\tau_{free} < \tau_{fluc}$). Therefore, these chains will have to associate and dissociate several times before being completely relaxed. This mechanism, which was experimentally observed in ref 38, is important because it allows obtaining a large relaxation times spectrum with telechelic polymers, even if their associating time is much longer than the fluctuation times of a free branch (i.e., $\tau_{associated} \gg \tau_{fluc}$, $\tau_{free} < \tau_{fluc}$). On the contrary, telechelic polymers in solution or weakly entangled, that is, characterized by a fast relaxation of a free branch ($\tau_{associated} \gg \tau_{fluc}, \tau_{free} > \tau_{fluc}$), will necessarily show a Maxwell relaxation.

On the basis of these arguments, we describe our approach in detail below.

III.1. Association Process. First, the association process of a functionalized group must be described. It consists of two average times: the "association" time, $\tau_{associated}$, which describes how long, on average, a pair of telechelic chain ends remains associated and the "free" time, τ_{free}, which describes how long, on average, a unassociated end chain will stay free before being again associated to another chain end. For a given chain end at a given time, t_i, from these two parameters and from its association status at the previous time step, t_{i-1}, we can determine the probability of whether it is associated with t_i[13]

$$p_{as-as}(t_{i-1}, t_i) = \exp\left(\frac{-(t_i - t_{i-1})}{\tau_{associated}}\right) \quad (1)$$

$$p_{as-free}(t_{i-1}, t_i) = 1 - p_{as-as}(t_{i-1}, t_i) \quad (2)$$

$$p_{free-free}(t_{i-1}, t_i) = \exp\left(\frac{-(t_i - t_{i-1})}{\tau_{free}}\right) \quad (3)$$

$$p_{free-as}(t_{i-1}, t_i) = 1 - p_{free-free}(t_{i-1}, t_i) \quad (4)$$

where $p_{as\text{-}as}$ and $p_{as-free}$ are the probabilities of an associated chain end to remain associated or to become free at the next time step and $p_{free-free}$ and $p_{free-as}$ are the probabilities of a free chain end to remain free or to become associated at the next time step. Whereas each extremity of a molecule is alternating between associated and unassociated status, the overall fraction of associated chain ends in the polymer is a constant, named $\Phi_{associated}$. This value is actually the fraction of chain ends in the "equilibrated" solution (i.e., at time $t \gg \tau_{associated}$), $\Phi_{associated}$, and is determined by calculating the fraction of associated chain ends at time t_i, knowing that at time t_{i-1} this fraction was equal to the same, $\Phi_{associated}$

$$p_{as}(t_i) = \Phi_{associated} p_{as-as}(t_{i-1}, t_i) + (1 - \Phi_{associated}) p_{free-as}(t_{i-1}, t_i) \quad (5)$$

Imposing that the above probability is equal to $\Phi_{associated}$, we find

$$\Phi_{associated} = \frac{p_{free-as}(t_{i-1}, t_i)}{1 - p_{as-as}(t_{i-1}, t_i) + p_{free-as}(t_{i-1}, t_i)} \quad (6)$$

As described in Section IV.3., this value is usually higher than 90% for telechelic systems.[19]

III.2. Fluctuation Times. The discussion that follows in this section primarily concerns telechelic stars. (The presence of unassociated branches is taken into account in Section III.5.) The telechelic samples that are studied in this work are monodisperse polymers, with all arms of the same molecular weight, and the same probability of being associated. Therefore, we assume that the fluctuation times of the molecular segments along an arm are identical for every branch with a telechelic end group.

We define here the fluctuation time as the time necessary for a free arm segment to relax by CLF. The fact that the arm relaxation is not allowed when its extremity is associated is taken into account in another term, which will be discussed later. Given this definition, the fluctuation times of the molecular segments of a star arm, localized by the normalized variable x (going from 0 at the extremity of the chain to 1 at the middle), can be described as for a regular star polymer, that is, by combining early and activated fluctuations processes. As explained in ref 56, the early fluctuations process describes the relaxation of the tube segments localized at the extremities of the chains and which require a low retraction potential ($x < x_{tr}$, $U(x_{tr}) = kT$). For deeper fluctuations, activated fluctuations must be used, ensuring the continuity between these two processes

$$\tau_{early}(x) = \frac{9\pi^3}{16}\left(\frac{M_a}{M_{e,0}}\right)^2 \tau_{R,chain} x^4 \quad \text{for} \quad x < x_{tr} \quad (7)$$

$$\tau_{fluc}(x) = \tau_{early}(x_{tr}) \exp\left(\frac{U(x) - U(x_{tr})}{kT}\right) \quad \text{for} \quad x < x_{tr} \quad (8)$$

$$\frac{\partial U(x)}{\partial x} = 3\left(\frac{M_a}{M_{e,0}}\right) x \Phi(x)^{\alpha} \quad (9)$$

where $M_{e,0}$ is the molecular weight between two entanglements, M_a is the molecular weight of an arm, and $\tau_{R,chain}$ is the Rouse time of an arm. One way to account for CR effects is to consider the dynamic tube dilution (DTD) process because of the action of the relaxed parts of the arms at a given time as effective solvents for the unrelaxed ones. Indeed, in eq 9, we account for the effective molecular weight between two entanglements, $M_e(t)$, which is defined as being

equal to $M_{e,0}/\Phi(x)^{\alpha}$, with $\Phi(x)$ being the arm fraction that is not considered as a solvent at the time when the segment x is relaxing[57,58] and α being the dilution exponent, which represents how effective this dilution effect is. As in our previous works,[55] it has been fixed to 1, considering entanglements as binary events. Defining $\Phi(x)$ in the case of a telechelic monodisperse polymer is not a trivial task. At very long times, that is, when all arms have already changed several times their association status, the usual assumption, which is based on the fact that fluctuation times are exponentially separated along the branch and according to which the same arm fraction is relaxed for each arm of same molecular weight, is valid. Therefore, as for a nonfunctionalized monodisperse star polymer, $\Phi(x)$ can be approximated by $(1 - x)$. However, at shorter times, the time during which a star arm was not associated can vary substantially from one star to another. Therefore, the polymer fraction, which does not act as a solvent, is not necessarily equal to $(1 - x)$. Nevertheless, because at these times the fluctuations of the branches are mainly described by the early relaxation process (eq 7), which does not depend on the DTD, approximating $\Phi(x)$ by $(1 - x)$ does not significantly affect the results.

Note that one could consider defining the unrelaxed polymer fraction as being equal to the polymer fraction, $\Phi_{associated}$. However, this approach is not correct because it does not account for the dynamics of the association process, that is, the fact that for well-entangled telechelic polymers the association status of each arm could have changed several times on the observed time scale. In particular, because the values of $\Phi_{associated}$ are generally higher than 90%, the fluctuation times of a "free" star polymer with long arms (for example, sample PI12-40, Table 1) are predicted to be much longer than by accounting for the telechelic association of the branches.

III.3. Association Process. *"Equilibrated" Solution.* Starting from the fluctuation times of the different segments along an arm, the easiest way to account for an associated arm that is not able to relax is by rescaling the time to consider only the fraction of time during which the chain end was unassociated, that is, free to move. Therefore, at a specific time, t, only a fraction $(1 - \Phi_{associated})$ of this time, t, is considered in the calculation of the survival probability of a segment x along the arm

$$p_{fluc}(x,t) \propto \exp\left(\frac{-(1-\Phi_{associated})t}{\tau_{fluc}(x)}\right) \tag{10}$$

However, as will be discussed in Section IV.3 below, this expression is only valid for $t \gg \tau_{associated}$, that is, when each arm has been already associated and free several times. At shorter times, the association−dissociation process of each arm must be accounted for at each time step because at the next (small) time step, a free-end arm (or chain) will not have the same probability of becoming associated as a chain-end that was already associated. (See eqs 1 and 4.) In the same way, a free chain end will not have the same probability as an associated chain end to be free. (See eqs 2 and 3.)

From the above, it becomes evident that considering the "equilibrated" solution represents a fast way to determine the ratio between τ_{free} and $\tau_{associated}$ and thus to fix one of the two degrees of freedom in the problem. By comparing model predictions and experimental data, only one value of the ratio $\tau_{free}/\tau_{associated}$ can make the model to capture the terminal regime correctly.

III.4. Association Process. *Times before the "Equilibrated" Solution.* Before the "equilibrated" solution, that is, at times smaller or similar to $\tau_{associated}$, we need to follow the association past of each arm. Furthermore, it is crucial to consider very small time steps, much smaller than τ_{free}, in order not to miss important information about the disassociation process and hence obtain results independent of the choice of this time step. This last condition has a large influence on the calculation time required for determining the rheological behavior of telechelic systems. Indeed, the relaxation modulus, $G(t)$, must be calculated over several orders of magnitude in time with a very small, linear time step.

To reduce the calculation time, we make two simplifications: (i) At a specific time, the survival−fluctuation−probability of a segment will depend on the *total* time during which the observed arm has been free to move and not on the sequence between its association and dissociation status. This allows summing-up the "free times" of an arm without keeping account of its exact associating history. (ii) As a consequence of part i, only the association status at the last time step t_{i-1} must be known to predict the new status of a chain end at time t_i. (See eqs 1−4.)

Without these considerations, the number of arms having a different past history would increase by a factor of two at each time step (because each of them can become associated or free). However, now two arms with the same previous association status and the same total "free" time can be grouped, which considerably reduces the number of different arms to consider.

On the basis of the above, the different association−dissociation histories for the arms are stored in a three-column matrix, **M**, in which each line i is related to arms that, in total, have been free to move during the same time and have the same associating status at the last time step. Their proportion is described in the first column, whereas the second column gives this total free time during which the arms were dissociated and the third one represents the association status of the arms at the last time step considered. Including the CR effect, which involves the rescaling of M_e on the global scale of the polymer (in addition to its influence in eq 9), the relaxation modulus is therefore expressed as

$$G(t) = G_N^0\left(\sum_i \mathbf{M}(i,1)\left(\int_0^1 p_{fluc,\,i}(x,t)\,dx\right)\right)^{1+\alpha} + G_{Rouse}(t) \tag{11}$$

with

$$p_{fluc,\,i}(x,t) = \exp\left(\frac{-\mathbf{M}(i,2)}{\tau_{fluc}(x)}\right) \tag{12}$$

where G_N^0 is the plateau modulus of the polymer, α is the dilution exponent, and $G_{Rouse}(t)$ takes into account the high-frequency Rouse contribution.[55] Because it is updated at each time step, the matrix **M** is also a function of time.

III.5. Unassociated Polymer Branches. In addition to the telechelic star arms, the possibility of having unfunctionalized end groups in the polymer must be considered. Indeed, from the synthetic procedure, there is always a possibility of having a small fraction of unfunctionalized star arms, which can lead to a small fraction of incomplete supramolecular structures. To test the influence of a small fraction of unfunctionalized arms, we can extend the above approach by considering a blend of telechelic and nonionic arms of identical molecular weight. From eqs 11 and 12, this modification is nearly direct because it requires only the addition of a term for the nonionic arms. However, the polymer

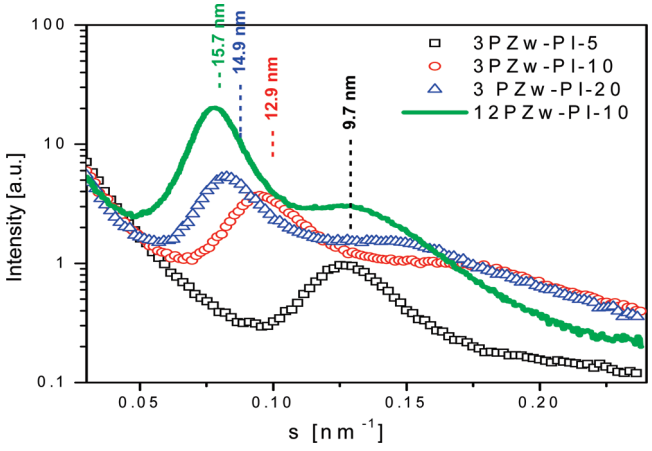

Figure 2. Total SAXS intensity profiles (intensity against the scattering wavevector $s = q/2\pi$) for telechelic three-arm polyisoprene stars indicating the effect of the arm length. The effect of the number of arms (functionality) is shown by comparing the SAXS intensity profiles of the telechelic star polyisoprenes 3PZw-PI-10 and 12PZw-PI-10, having the same arm molecular weight.

fraction that does not act as a solvent, $\Phi(x)$, used in eq 9 for determining the fluctuation times of the molecular segments along the arms, must be modified accordingly. Because the relaxation times of a nonionic arm and a telechelic arm differ by several orders of magnitude (as assumed in the modeling), we have assumed that the telechelic arms are still oriented during the relaxation of the nonionic arms (thus the unrelaxed part of the polymer, knowing that a branch of a nonionic arm is relaxed until x_{branch}, $\Phi(x_{branch}) = \upsilon_{telechelic} + (1 - \upsilon_{telechelic})(1 - x_{branch})$, with $\upsilon_{telechelic}$ the volumetric fraction of telechelic branches) and that the nonionic arms are fully relaxed when the relaxation of their telechelic counterparts starts (thus the unrelaxed part of the polymer, knowing that a branch of a telechelic arm is relaxed until $x_{telechelic}$, with $\Phi(x_{telechelic}) = \upsilon_{telechelic}(1 - x_{telechelic})$.

IV. Results and Discussion

IV.1. Structural Features. Figure 2 depicts the SAXS intensity as a function of the scattering wave vector, s, for the three telechelic three-arm polyisoprene stars of various molar masses. The observed scattering effect results primarily from the aggregation of the functional groups into microdomains, which constitute areas of electron density contrast with respect to the polyisoprene matrix. The broad but intense peaks accompanied by less-intense second-order intensity maxima indicate relatively well-defined spatial correlations of these aggregates but do not allow for more detailed assignments concerning their forms and types of spatial order. The ratios between the positions of the first and second peaks are equal to 0.6, 0.54 and 0.55 for 3PZw-PI-5, 3PZw-PI-10, and 3Pzw-PI-20, respectively. We characterize the size scale of the ordering (or correlation length, d_{peak}) by taking into account the positions of the first intensity maxima (s_{peak}): $d_{peak} = a/s_{peak}$ (where $a = 1.23$ for a structure controlled by two-body correlations).[47,59,60] This size is considered to be the distance between nearest neighboring centers of ordered entities, that is, clusters of functional groups, and is of a different origin than the order that has been observed in nonionic analogues such as multiarm star polymers[59] and block copolymer micelles.[61] Indeed, here it is due to scattering of the zwitterionic groups (which aggregate), in contrast with the cores of nonionic stars and block copolymer micelles. Consequently, the latter can form a liquid-like order where the particle centers are in cubic arrangements, whereas in the present case, it is the junctions that are arranged accordingly. This order could be compared with the ordering of other telechelic stars (three-arm stars),[47] albeit only qualitatively (i.e., formation of aggregates) because here the study of supramolecular assembly refers to systems with different functionality, molar mass, and strength of dipolar groups. It is interesting that these values of d_{peak} (Figure 2) conform to $d_{peak} \approx M_a^{0.33}$, as reported before for other star systems in the melt.[59] Here this correlation may suggest that the aggregates independently of the arm lengths consist of nearly the same number of functional groups. The correlation distances determined from the SAXS results provide the possibility of extracting the aggregation number of the ordered zwitterionic domains; each of these clusters is considered on average as a dense object with volume $V = d_{peak}^3 = nN_{star}\upsilon$, where n is the aggregation number, N_{star} is the degree of polymerization of the star, and $\upsilon = m/\rho N_A$ is the segmental volume (m is the molecular mass of the monomer, ρ is the polymer mass density, and N_A is the Avogadro number). Indeed, for the three samples with the three-arm stars 3PZw-PI-5, 3PZw-PI-10, and 3PZw-PI-20, we find nearly the same n, that is, 27, 32 and 25, respectively. This implies that the star molar mass affects the correlation length of the clusters, but their aggregation number appears to be controlled primarily by the electrostatic attractions, at least for the range of molar masses investigated. The latter does not seem to conform to the findings of recent dilute solution studies, which suggest that there is a tendency for reduced aggregation number with increasing arm molar mass because of excluded volume effects.[53] However, there may be a quantitative difference (for instance, the threshold molecular weight for observing the reduction in aggregation number) between solutions and melts.

The effect of the number of arms for stars of the same arm molecular weight on their ordering is also depicted in Figure 2, where the SAXS intensity profiles are plotted for 3PZw-PI-10 and 12PZw-PI-10. Here it is evident that whereas the features of liquid-like order remain, increasing the functionality leads to stronger order with larger correlation length. The ratios between the position of the first and second peaks are equal to 0.54 and 0.62 for 3PZwPI-10 and 12PzwPI-10, respectively. From these data, the extracted apparent aggregation number varies from 32 to 18 as the functionality is increased from 3 to 12. The implication is that the formation of stable aggregates primarily depends on the number of dipolar groups and the reduced entropy due to increased functionality (especially near the star center) and not so much on the possible stereochemical hindrance due to the size of the arms (as demonstrated in Figure 2). This finding is consistent with experimental observations from three-arm stars end-capped with sulfozwitterion groups, where the stars with all arms functionalized had a smaller degree of association.[47] In this context, we mention the relevant work of Likos of coworkers[24−26] who studied the association behavior of telechelic star solutions as function of the effective size and strength of the end groups and volume fraction. For low-functionality stars, the watermelon type of structures was reported. From the above discussion, intramolecular associations in the case of 12-arm stars cannot be excluded. Note that these features were unchanged after long annealing (on the order of 24 h). However, recent work suggests that these systems may change (at least in the intermediate time range associated with association−dissociation balance) over much longer periods.[29]

IV.2. Rheology. Figure 3 shows the mechanical spectra of three telechelic three-arm star polyisoprenes with varying arm molar mass. These master curves represent dynamic

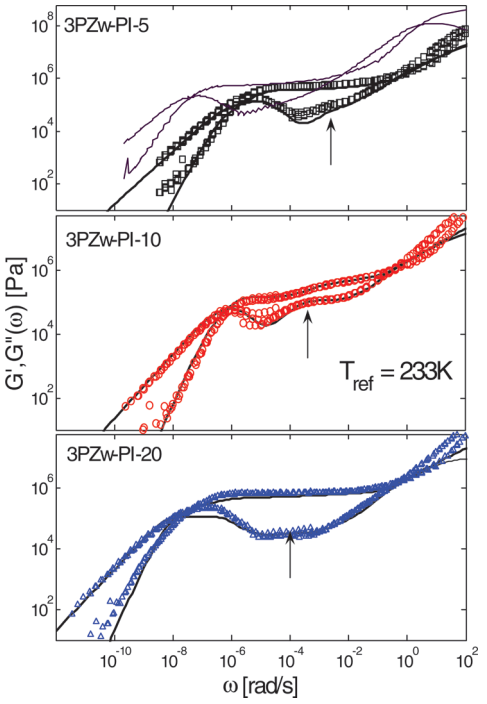

Figure 3. Effect of arm length on the linear rheological response (frequency master curves at references temperature T_{ref} = 233 K) of the telechelic three-arm polyisoprene star melts. The terminal region is characterized by the slopes 1 and 2 for G'' and G', respectively. The arrow indicates an extra relaxation peak, corresponding to the relaxation of the unassociated branches. The thin curves for sample 3PZw-PI-5 represent the initial data before shifting them in such a way that the high-frequency dynamics become the same as that with the other samples. The bold curves represent the predicted storage and loss moduli.

frequency sweeps referring to a temperature T_{ref} = 233 K. All three samples exhibit nearly the same plateau modulus, which has been estimated to be 5.7×10^5 Pa. This value was used in the modeling (discussed in Section IV.3) and is relatively large compared with the plateau modulus of unfunctionalized linear polyisoprene samples (about 4.5×10^5Pa).[62,63] This is attributed to the presence of junctions and the formation of clusters due to the dipolar groups (as discussed below). Such an increase in the plateau modulus has already been observed with other telechelic systems[29] and is discussed in Section IV.3. The samples flow at low enough frequencies, virtually following the classic Newtonian terminal scaling $G' \approx \omega^2$ and $G'' \approx \omega$. The terminal relaxation times of these functionalized stars are, however, much longer than the corresponding times of the unfunctionalized stars with the same arm molar masses. This is attributed to the temporary trapping of the functionalized arm ends in clusters, which were detected by the SAXS. The observation of flow of the systems at long times, in the range of temperatures for which the cluster presence has clearly been observed by temperature-dependent SAXS measurements (up to 100 °C for 3PZw-PI-10, as seen in Figure 4), indicates that the clusters are transient structural units (much like other telechelic or surfactant self-assemblies) with a certain lifetime that is related to the probability with which a single arm can escape a cluster to take part in the observed flow of the star. (Also see the Modeling Consideration section.) Such a picture suggests that there could be two possible states of the functionalized arms, trapped in the clusters and free (intermittent) state.

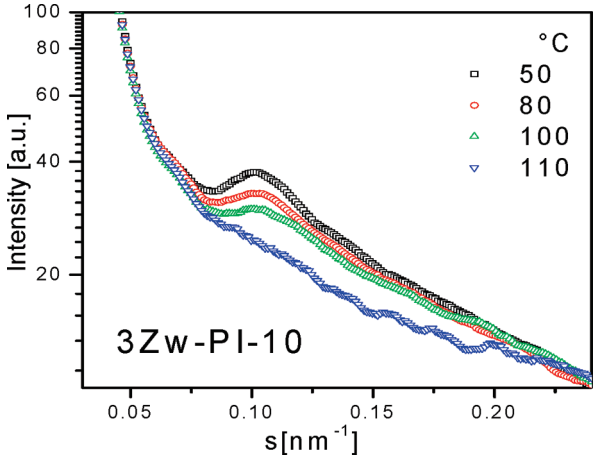

Figure 4. Temperature-dependent SAXS measurements with 3Zw-PI-10 sample in the range of 50−110 °C.

As observed with most of the telechelic systems,[29,47,48,64−67] these samples show a thermorheological complexity around the minimum of the loss modulus, that is, when the chains start to escape from the telechelic junctions (see also Figure 5). This process depends on the strength of the junction and the temperature. However, depending on the chemistry of the dipolar group (and not the arms), this mechanism is not expected to exhibit the same temperature dependence with the relaxation time of an entanglement segment, τ_e. Therefore, the motions of these telechelic polymers are governed by two different mechanisms (dissociation and disentanglement) with two different "internal clocks" ($\tau_{associated}$ and τ_e). Before the chains escape from the junctions, the dynamics of the entanglement segments (τ_e) is the only mechanism at place, and the sample shows a thermorheologically simple behavior. At low-enough frequencies corresponding to the "equilibrated" solution (Section III), there is a need to account for the temperature dependence of both the disentanglement and the dissociation processes. In this region, the association−dissociation process slows down the relaxation of the polymer but does not alter the shape of its rheological curves. The sample can exhibit a thermorheologically simple behavior. Experimental results from literature support this scenario.[29,47,48,64−67] It was recently shown that the relaxation moduli in this low-frequency region present the same shape as the ones of the unfunctionalized analogue polymer but shifted to lower frequency.[29] At intermediate frequencies, where eq 10 is not yet valid, the temperature dependence cannot be easily described because the relaxation status of the molecules changes. This leads to the thermorheological complexity of the sample in this frequency region.

Furthermore, as shown in Figure 3, in this frequency range, a secondary relaxation is observed, which leads to a small shoulder in the loss modulus curve (samples 3PZw-PI-10 and 3PZw-PI-20). As indicated in ref 29, this relaxation depends on the annealing time and is considerably reduced when the system is fully equilibrated after long time. On the basis of the model analysis (Section IV.3), we can show that the corresponding relaxation relates to the arms that are not able to associate and hence are not in equilibrium (because on average, the probability for a telechelic end to be associated is equal to 99%). For the samples presented in this work, the average fraction of such arms is ∼12% (Section IV.3, and Table 2), apart from sample 3PZw-PI-10, which exhibits a large amount of unassociated branches (50%). The annealing time of this latter sample was probably not long enough.[29] Note that among these free arms, one could also find a small fraction of unfunctionalized branches.

Table 2. Survival Time of a Free Telechelic End Group, τ_{free}, Survival Time of a Telechelic Junction, $\tau_{associated}$, and Volumetric Fraction of Unassociated Branches (free arms)

	τ_{free} (s)	$\tau_{associated}$ (s)	Free arms (%)
3PZw-PI-5	10	10^5	20
3PZw-PI-10	700	10^6	50
3PZw-PI-20	200	$2.5\ 10^6$	15

	τ_{free} (s)	$\tau_{associated}$ (s)	Free arms (%)
12PZw-PI-10	9	10^6	13
12PZw-PI-45	700	10^6	5

Both cases (unfunctionalized or out-of-equilibrium) must be taken into account in the modeling part. (See Sections III and IV.3.)

An additional remark here concerns the segmental dynamics and, in particular, the glass transition ($G'-G''$ high-frequency crossover), which is influenced by the arm molar mass. In particular, the sample 3PZw-PI-5 shows a much slower segmental dynamics than samples 3PZw-PI-10 and 3PZw-PI-20. (See the thin lines in Figure 3.) This is in agreement with the glass-transition temperature (T_g) values determined using DSC. (See Table 1.) The T_g increases with decreasing chain length, which is opposite to behavior of melts of nonionic chains with corresponding length.[68] In general, a star has a T_g very close to that of a linear chain, which increases with molar mass and remains constant for high molar masses.[68−70] In the present situation, two reasons can be considered to be responsible for the observed effect: (1) the use of polar initiator containing dimethylamine group in the synthesis affects the microstructure of polyisoprene, increasing the amount of 3,4-content,[40,53,54,71] and (2) the decrease in arm length increases the number of chemical and physical "cross-links" created in this system by the star centers and the phosphoro-zwitterions aggregation, respectively. The microstructure of the amine-capped precursors used for the synthesis of the telechelic linear and star polyisoprenes is given in Table 3. The 3,4-content is found to be much higher than that with nonionic polyisoprene sample because of the fact that polar groups change the microstructure of polydienes.[35,47]

The T_g dependence on microstructure was studied by Graessley et al[71] for polyisoprenes and hydrogenated polyisoprenes, showing a quadratic dependence of T_g on the 3,4-content. On the basis of these results, we estimated the T_g value of the three-arm star with the smallest arms (PI-5 in Table 3) to −40 °C. Because the significance of both effects (1) and (2) is reduced for the longer star arms, the glass transition of 3PZw-PI-20 is close to the linear polyisoprene, and that of 3PZw-PI-10 is only weakly increased, as confirmed by the T_g values reported in Table 1. We expect a larger effect of the microstructure for sample 3PZw-PI-5, which contains a large raction of 3,4 microstructure.[35,71] This is indeed reflected in its segmental dynamics, as demonstrated in Figure 3, where the $G'-G''$ crossover in the high-frequency Rouse regime appears at much lower frequency than for the samples 3PZw-PI-10 and 3PZw-PI-20. This effect should be taken into consideration when comparing times by accounting for the isofrictional relaxation times.

The latter point is confirmed in Figure 5, which shows the master curves of linear and star (2, 3, and 12 arms) phosphoro-zwitterionic end-capped polyisoprenes with the same arm molar mass. It is evident from this Figure that the glass transition in the three cases is approximately the same, as expected based on the above argumentation. Moreover, this Figure demonstrates that the effect of increasing arm functionality is severely slowing down the dynamics, presumably because of the corresponding larger cluster size. (See also the Discussion in the next section.) It is also interesting to note in this respect that the separation between the broad G'' maximum and the $G'-G''$ crossover is more pronounced in the 12-arm star case; this separation relates to the wide range of arm relaxation modes, where in the present

Table 3. Microstructure of the Precursors for the Synthesis of the Telechelic Linear and Star Polyisoprenes Described in Table 1 from (Ref 53)

	M_a [g/mol]	1,4 wt %[a]	3,4 wt %[a]
PI-5	5100	66	34
PI-10	10 000	78	22
PI-20	20 000	81	19
PI-40	41 700	89.5	10.5
PI-100	104 800	93	7

[a] Determined by ^{1}H NMR in $CDCl_3$

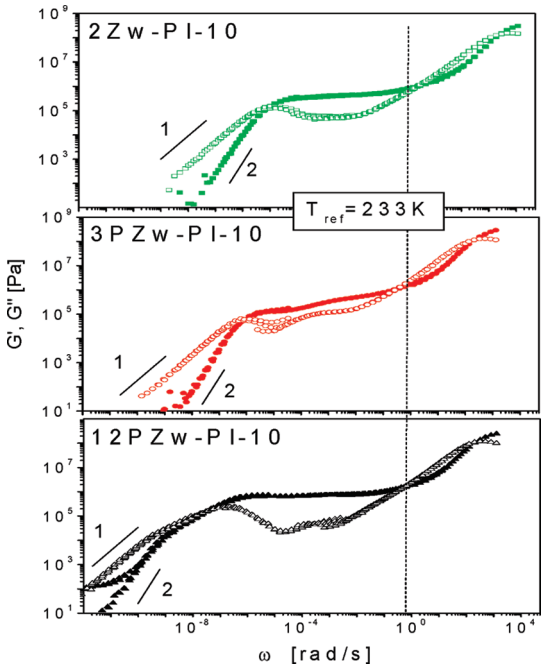

Figure 5. Master curves (at T_{ref} = 233 K) for the polyisoprene melts, linear, and star with different arm numbers, having the same arm molar mass M_a = 10 000 g/mol.

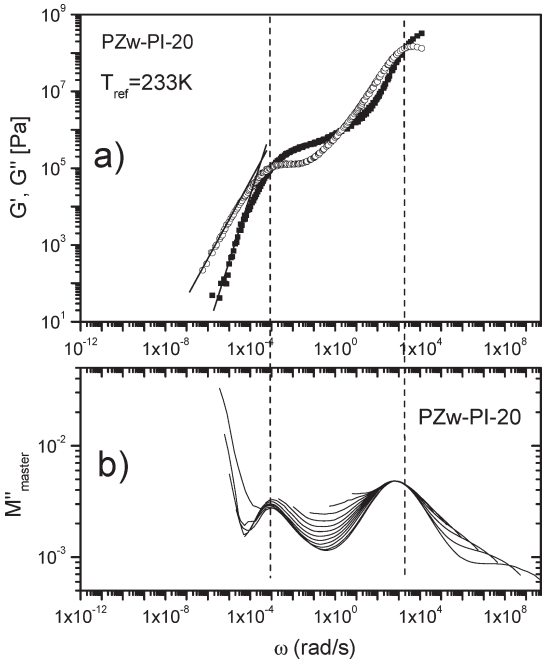

Figure 6. Comparison of (a) mechanical and (b) dielectric master curves (at T_{ref} = 233 K) of linear semitelechelic PZw-PI-20, indicating the high-frequency segmental and low-frequency terminal relaxations. The curves in part b built from data at different temperatures (from 153 to 373 K) show a large thermorheological complexity.

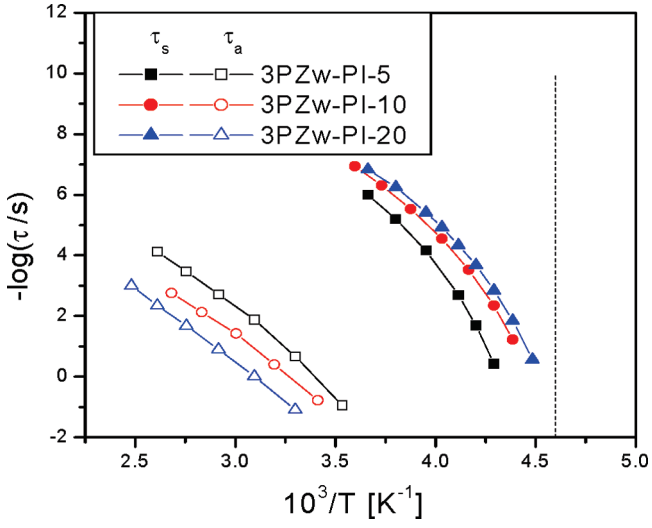

Figure 7. Dielectric data of the temperature dependence of the segmental (τ_s) and terminal (τ_a) relaxation times for the three-arm stars with various arm lengths. The vertical dashed line identifies the T_g of the linear 1,4-polyisoprene (−55 °C).

situation, the arm is considered to be a segment between two junction points (star center, dipolar association) and the concentration of junctions (related to a specific molecule) is larger for the 12-arm star. Also note that the semitelechelic linear sample exhibits a relatively fast relaxation, which is due to the fact that it should be able to relax always because of its free end.

Dielectric spectroscopy is particularly useful for studying the molecular motions of polyisoprene because it reveals both the end-to-end chain motion (normal mode) and the short-time scale motion (segmental mode). Its complementarity to the mechanical spectroscopy is demonstrated in Figure 6, which depicts the (a) mechanical and (b) dielectric spectra of the semitelechelic linear PZw-PI-20. This Figure also confirms the interpretation of the rheological findings above. Figure 7 depicts the respective terminal (τ_a) and segmental (τ_s) relaxation times for telechelic stars with three arms and different arm molar masses. The results, presented in the form of an activation plot, support the observed effect of arm molar mass on the segmental motion and the respective slow terminal region. In agreement with the rheological data of Figure3, we observe a slowing-down of the segmental dynamics with decreasing their arm molecular weight, which is due to their different microstructure[71] (Table 3). On the other hand, the finding that increasing M_a yields slower terminal relaxation appears to be a consequence of the fact that the flow of the star depends on: (i) the probability of belonging to a cluster (i.e., on the lifetime of a free telechelic junction, the lifetime of an associated junction depending only on the strength of the electrostatic attractions, which is independent from M_a), as already mentioned and (ii) the size of the star, which depends on the M_a (much like the arm relaxation in unfunctionalized stars) and is further discussed in the next Section.

IV.3. Quantitative Analysis. *Material Parameters and Survival Times.* To predict the linear viscoelasticity of telechelic polymers, we need first to define the three material parameters relative to tube models, that is, the plateau modulus, G_N^0, the molecular weight between two entanglements, M_e, and the Rouse time of an entanglement segment, τ_e.[72] As already mentioned, the value of G_N^0 at −37 °C was fixed to 5.7×10^5 Pa, a value slightly larger than the plateau modulus of unfunctionalized polyisoprene samples,[62,63] possibly because of the presence of telechelic junctions, which increases the effective cross-link density of the samples and forms clusters.[29] On the basis of this representation, the value of the plateau modulus should slightly increase with the density of clusters, that is, with decreasing the molar mass of the star arm. This is indeed observed in Figures 3 and 8, where the larger discrepancy between the predicted and the experimental plateau modulus is observed for sample 3PZw-PI-5, whereas for sample 12PZw-PI-40 the agreement is very good. However, it is difficult to quantify this effect, which is relatively small. Therefore, we preferred keeping a constant value for describing the plateau modulus. The molar mass between two entanglements, M_e, was fixed to 3800 g/mol. Considering a density of 0.89 g/mol at −40 °C (using a temperature-dependent density of polyisoprene, $\rho = 0.86431 - 0.00054441*T$),[73] this is within the 15% of the $G_N^0 - M_e$ relationship ($G_N^0 = 4\rho RT/5M_e$). The Rouse time of an entanglement segment, τ_e, was fixed to 12s at −40 °C. To compare theoretical and experimental results, the experimental data were horizontally shifted for suppressing the effect of the different T_g values of the samples (Table 1) and thus for ensuring that all samples present the same high-frequency Rouse dynamics.[74]

As discussed in Section III, to predict the rheology of telechelic polymers, the lifetime of a telechelic junctions $\tau_{associated}$ as well as the lifetime of a free chain end, τ_{free}, must be defined. To obtain an idea about their values, these times were first estimated via a best fitting procedure for each sample. Then, for a rigorous determination of $\tau_{associated}$ and τ_{free}, we first considered the "equilibrated" solution in the terminal regime (Section III), which provided the ratio between the two lifetimes. As shown in Figure 8a, by varying the values of $\tau_{associated}$ and τ_{free} while keeping their ratio constant, results in a wide range of rheological behavior from the "equilibrated" solution (if $\tau_{associated}$, $\tau_{free} \ll \tau_{fluc}$), according to which a large fraction of the polymer is already relaxed at intermediate frequencies (around 10^{-4} rad/s),

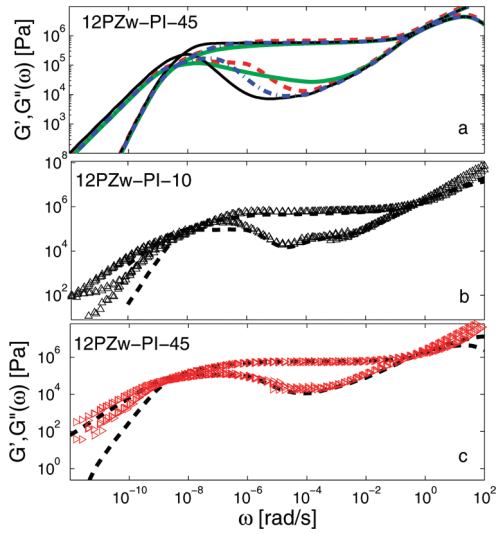

Figure 8. (a) Predicted storage and loss moduli for sample 12PZw-PI-45. Results are obtained by fixing the ratio $\tau_{free}/\tau_{associated} = 7 \times 10^{-4}$, and by considering either the "equilibrated" solution (green, thick —), or the full model with $\tau_{free} = 7 \times 10^2$ s (red, ---), with $\tau_{free} = 7 \times 10^3$ s (blue, -.-), or with $\tau_{free} = 7 \times 10^4$ s (black, thin —). (b,c) Comparison between theoretical (---) and experimental (symbols) storage and loss moduli for the 12-arm stars with various arm lengths.

to a Maxwell description (if $\tau_{free} > \tau_{fluc}$), according to which an arm is considered relaxed as soon as it becomes unassociated. For the present experimental systems, the arms are well-entangled and have relatively long relaxation times. Therefore, the disentanglement mechanism competes with the dissociation process, and the switch between associated and unassociated state must occur several times before the complete relaxation of a molecule. This leads to a broader terminal relaxation peak of the loss modulus, in accord with the experimental observations.

As expected, all curves in Figure 8a superimpose at low frequencies ($\omega \ll 1/\tau_{free}$, $1/\tau_{associated}$) because they are characterized by the same ratio $\tau_{free}/\tau_{associated}$. (See Section III.) Knowing the $\tau_{free}/\tau_{associated}$ ratio, the exact value of the unassociated and associated times are easily determined because, as shown in Figure 8a, the shape of their relaxation peak is very sensitive to these values. These two times are considered here to be best-fit parameters, and their different values are presented in Table 2 for the telechelic star polymers. Apart from the sample with very short arms (3Zw-PI-5), all samples have very similar values of $\tau_{associated}$. This is consistent with the fact that this survival time should mainly depend on the chemistry of the telechelic bond as well as on the aggregation number of the ordered zwitterionic domains, which are very similar for the different polymers. (See Section IV.1).

The time during which an unassociated arm end stays free, τ_{free}, strongly varies depending on the arm molar mass and the star functionality and hence on the mobility of the arm. Also note that for all samples, the ratio $\tau_{free}/\tau_{associated}$ is very small. This ensures that on average more than 99% of the chain ends remain associated.

IV.4. Model Predictions. *Telechelic Star Polymers.* The predictions obtained for the 3-arm and the 12-arm star telechelic polymers are compared against the experimental data in Figures 3 and 8, respectively. The small peak that appears in the G'' curves in the intermediate region and that corresponds to a small fraction of unfunctionalized arms or arms in intermittent situation (not associating with neighboring groups[29]), has been taken into account in the model. As discussed in Section III, it corresponds to a small polymer fraction, relaxing much faster than the telechelic star molecules. The fraction of free arms considered with the different samples is described in Table 2 and has been fixed by best-fitting procedure. The different value of 3PZw-PI-10 explains why the viscoelastic curves of this sample are quite different from the other ones, showing two distinct relaxation peaks in the loss modulus curve.

As shown in Figure 3, the model captures very well the experimental data of the three-arm telechelic star polymers, using only two parameters, $\tau_{associated}$ and τ_{free} (in addition to the fraction of unfunctionalized arms, see Table 2), and provides a clear picture of the association mechanism. This is mainly due to the fact that both disentanglement and dissociation processes are considered simultaneously, not accounting for the relaxation of an arm when it is associated. Accounting for these two "internal clocks" of the polymer, this model describes the rheological behavior, which differs from the simple Maxwell relaxation observed with telechelic samples, where arm relaxation is activated immediately after its dissociation (and characterized by $\tau_{fluc} < \tau_{free}$). This last case is mainly observed with short branches[38,75] or with telechelic polymers in solution.[12,19]

In Figure 8b,c, the predictions obtained for the 12-arm telechelic star polymers are compared with the experimental data. Results obtained are less accurate than with the three-arm star molecules. Indeed, in this case, an extra relaxation process is observed at very low frequency in the experimental data, which cannot be captured by the model. Whereas its origin is not clear, it is tempting to relate it to a similar terminal relaxation process observed with multiarm star polymers,[76] which was attributed to the relative motion of the center-of-mass of the stars. This was seen as a reflection of the colloidal nature of the stars, which feel an excluded volume on their own size scale, that is, caging.[60] This is indeed not taken into account in the model, according to which a telechelic star is relaxed as soon as its arms are disoriented. As explained in the literature, this colloidal feature is usually observed for star polymers with a higher functionality ($f > 30$).[26,76] However, as evidenced by the SAXS data (Section IV.1), the 12-arm star samples contain a larger amount of intramolecular associations, which could increase their colloidal character compared with the corresponding nonionic molecules.[2,26]

Semitelechelic and α,ω-Telechelic Linear Polymers. As shown in Figure 9 and discussed in the previous section, the relaxation of the semitelechelic linear sample PZw-PI-20 is fast compared with the corresponding telechelic star polymers. This is explained by the fact that when the telechelic extremity of a molecule is trapped in a cluster of zwitterionic bonds the other unfunctionalized extremity is free to move. Therefore, the semitelechelic molecule is always able to relax and, according to the theory, its relaxation can be described by two different processes: it relaxes as a star polymer with arms of molar mass $M_a = 20$ kg/mol when its functionalized chain-end is associated, and it relaxes as a linear chain (or a two-arm star polymer with $M_a = 10$ kg/mol) when it is unassociated. However, because the fluctuation time of an arm with $M_a = 20$ kg/mol is much shorter than the association time of the zwitterionic end, this sample effectively relaxes as a stable multiarm star polymer with $M_a = 20$ kg/mol and is composed of a core formed by the different zwitterionic bonds. (See Figure 9a.)

In Figure 9a, predictions obtained by considering this latter picture are compared with the experimental data. The agreement is very good, supporting our hypothesis. The extra relaxation process observed at low frequency in the experimental data is due to the above-mentioned

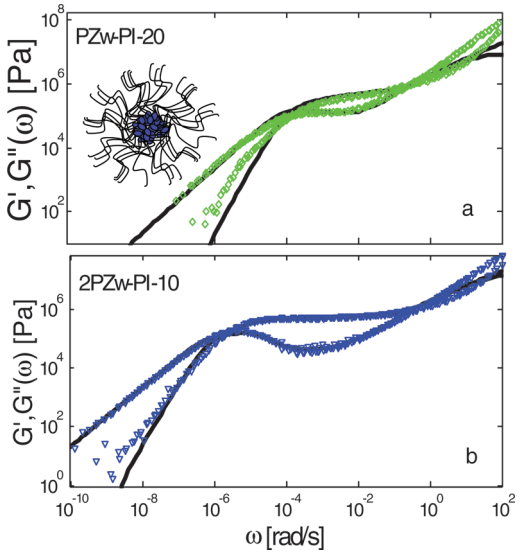

Figure 9. Comparison between theoretical (lines) and experimental (symbols) storage and loss moduli for the linear telechelic and semitelechelic samples.

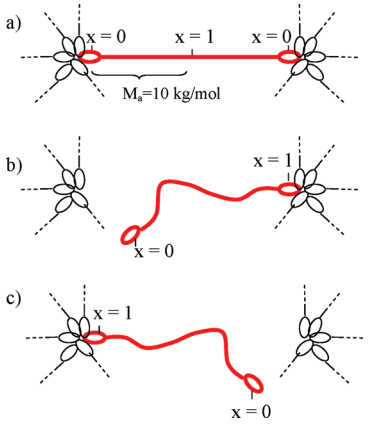

Figure 10. Cartoon representations of the relaxation of an entangled telechelic linear polymer. (a) Reference coordinate: a linear chain is considered as a two-arm star molecule. (b,c) When a telechelic group becomes unassociated, the linear chain relaxes as a branch of M_a = 20 kg/mol. Note that the probability of having the two telechelic end groups unassociated at the same time is negligible.

colloidal behavior of the core of these star structures[76] and cannot be taken into account in the model. On the other hand, the viscoelastic data of the telechelic linear sample 2PZw-PI-10 are shown in Figure 9b. Because their two ends are functionalized, these molecules relax much slower than the corresponding semitelechelic case. (See Figure 9a.) Because the probability for a chain to have two unassociated end groups at the same time is extremely small, we can neglect their relaxation by reptation and consider that they relax by CLF. Furthermore, because one end is fixed during the fluctuations of the other one, CLF must be related to the whole molecule, that is, to arms with M_a = 20 kg/mol (and not 10 kg/mol). This leads to a new, particular case, which is presented in Figure 10: the molecular segments are fluctuating in respect to the associated end group, that is, from $x = 0$ at the free extremity to $x = 1$ at the associated extremity, but a molecule is considered to be fully relaxed when the middle of the chain ($x = 0.5$) is disoriented, not the segment ($x = 1$).

This is due to the fact that CLF acts symmetrically from the two telechelic ends with same the probability, and thus the slower molecular segment is indeed the middle segment. The predictions obtained by considering that $\tau_{associated} = 10^5$ s and $\tau_{free} = 100$ s, are also presented in Figure 9b, in good agreement with the experimental data. Note however that the value considered for $\tau_{associated}$ is short compared with that of the other samples. (See Table 2.) This cannot be currently explained, and more data are needed in the future to investigate this issue.

V. Concluding Remarks

Phosphoro-zwitterionic polyisoprene star melts self-organize as a result of the dipolar interactions between the arms end groups, forming clusters whose sizes primarily depend on the number of dipolar groups per star. The clusters have a transient character because of the finite lifetime of the telechelic junctions. The respective dynamic response is characterized by the following features: (i) The segmental dynamics is affected by the telechelic functionalization, especially for short arm lengths, because of changing microstructure. (ii) The terminal relaxation is slower compared with similar nonionic stars and reflects considerably slower arm relaxation because it is now controlled by the probability of arm escape from the telechelic junctions (clusters); following this escape, the stars flow according to their size. However, additional slow modes are observed in higher-functionality stars or clusters from semitelechelic linear chain and attributed to the center-of-mass terminal motion of these objects. The relaxation of the arms can be described quantitatively with remarkable accuracy using a tube-based time-marching model, where the relative lifetime of dipolar associations is taken into account and in fact treated as the only adjustable parameter.

Acknowledgment. While this work was in progress, Tadeusz Pakula, a dear longtime colleague and friend, passed away. This last collaboration is dedicated to his memory. We are grateful to A. Miros for assistance with some measurements. Partial support has been received by the Greek Ministry of Education ("Polymer Science and its Applications" graduate program), the EU (network HUSC, HPRN-CT-2000-00017 and NoE Softcomp, NMP3-CT-2004-502235), and the Fonds National de la Recherche Scientifique to EVR. This manuscript was completed when D.V. was visiting the Laboratoire Matière Molle et Chimie at ESPCI in fall 2009 with the support of the "Chaire Michelin-ESPCI".

References and Notes

(1) Uraneck, C. A.; Hsieh, H. L.; Buck, O. G. *J. Polym. Sci.* **1960**, *46*, 535.
(2) Lo Verso, F.; Likos, C. N. *Polymer* **2008**, *49*, 1425.
(3) Torkkeli, M.; Serimaa, R.; Ikkala, O.; Linder, M. *Biophys. J.* **2002**, *83*, 2240.
(4) Muthukumar, M.; Ober, C. K.; Thomas, E. L. *Science* **1997**, *277*, 1225.
(5) Jenekhe, S. A.; Chen, X. L. *Science* **1998**, *279*, 1903.
(6) Brett, H.; Meijer, E. W. *Science* **2006**, *313*, 929.
(7) Kwon, G.; Naito, M.; Yokoyama, M.; Okano, T.; Sakurai, Y.; Kataoka, K. *J. Controlled Release* **1997**, *48*, 195.
(8) Kim, S. Y.; Shin, I. L. J.; Lee, Y. M.; Cho, C. S.; Sung, Y. K. *J. Controlled Release* **1998**, *51*, 13.
(9) Luman, N. R.; Kim, T.; Grinstaff, M. W. *Pure Appl. Chem.* **2004**, *76*, 1375.
(10) Frechet, J. M. J. *Science* **1994**, *263*, 1710.
(11) Vogtle, F.; Gestermann, S.; Hesse, R.; Schwierz, H.; Windisch, B. *Prog. Polym. Sci.* **2000**, *25*, 987.
(12) Pellens, L.; Ahn, K. H.; Lee, S. J.; Mewis, J. *J. Non-Newtonian Fluid Mech.* **2004**, *121*, 87.
(13) (a) Semenov, A. N.; Nyrkova, I. A.; Khokhlov, A. R. *Macromolecules* **1995**, *28*, 7491. (b) Semenov, A. N; Joanny, J-F; Khokhlhov, A. R *Macromolecules* **1995**, *28*, 1066.
(14) Kudlay, A.; Erukhimovic, I. *Macromol. Theory Simul.* **2001**, *10*, 542.

(15) (a) Kumar, S. K.; Panagiotopoulos, A. Z. *Phys. Rev. Lett.* **1999**, *82*, 5060. (b) Panagiotopoulos, A. Z.; Floriano, M. A.; Kumar, S. K. *Langmuir* **2002**, *18*, 2940.
(16) Kumar, S. K.; Douglas, J. F. *Phys. Rev. Lett.* **2001**, *87*, 188301.
(17) Weiss, R. A.; Zhao, H. Y. *J. Rheol.* **2009**, *53*, 191.
(18) Hurtado, P. I.; Berthier, L.; Kob, W. *Phys. Rev. Lett.* **2007**, *98*, 135503.
(19) (a) Rubinstein, M.; Semenov, A. N. *Macromolecules* **1998**, *31*, 1373. (b) Rubinstein, M.; Semenov, A. N. *Macromolecules* **1998**, *31*, 1386. (c) Rubinstein, M.; Semenov, A. N. *Macromolecules* **2001**, *34*, 1058. (d) Rubinstein, M.; Semenov, A. N. *Macromolecules* **2002**, *35*, 4821.
(20) Meng, X. X.; Russel, W. B. *Macromolecules* **2005**, *38*, 593.
(21) Nagarajan, R.; Ruckenstein, E. *Langmuir* **1991**, *7*, 2934.
(22) (a) Leibler, L.; Rubinstein, M.; Colby, R. H. *Macromolecules* **1991**, *24*, 4701. (b) Leibler, L.; Rubinstein, M.; Colby, R. H. *J. Phys. II* **1993**, *3*, 1581.
(23) Kujawa, P.; Audibert-Hayet, A.; Selb, J.; Candau, F. *Macromolecules* **2006**, *39*, 384.
(24) Lo Verso, F.; Likos, C. N.; Mayer, C.; Lowen, H. *Phys. Rev. Lett.* **2006**, *96*, 187802.
(25) Lo Verso, F.; Likos, C. N.; Lowen, H. *J. Phys. Chem. C* **2007**, *111*, 15803.
(26) Lo Verso, F.; Panagiotopoulos, A. Z.; Likos, C. N. *Phys. Rev. E* **2009**, *79*, 010401.
(27) Marrucci, G.; Bhargava, S.; Cooper, S. L. *Macromolecules* **1993**, *26*, 6483.
(28) (a) Tabuteau, H.; Ramos, L.; Nakaya-Yaegashi, K.; Imai, M.; Ligoure, C. *Langmuir* **2009**, *25*, 2467. (b) Nakaya-Yaegashi, K.; Ramos, L.; Tabuteau, H.; Ligoure, C. *J. Rheol.* **2008**, *52*, 359.
(29) Stadler, F. J.; Pyckhout-Hintzen, W.; Schumers, J. M.; Fustin, C. A.; Gohy, J. F.; Bailly, C. *Macromolecules* **2009**, *42*, 6181.
(30) Khokhlov, A. R.; Philippova, O. E. In *Solvent and Polymer Self-Organization*; Webber, S, Ed.; Kluwer: Dordrecht, The Netherlands, 1996; pp 197−225.
(31) Muthukumar, M.; Ober, C. K.; Thomas, E. L. *Science* **1997**, *277*, 1225.
(32) Zimmerman, S. C.; Zheng, F.; Reichert, D. E. C.; Kolotuchin, S. V. *Science* **1996**, *271*, 1095.
(33) *Theoretical Challenges in the Dynamics of Complex Fluids*; McLeish, T. C. B., Ed.; NATO ASI *339*; Kluwer: London, 1997.
(34) Adachi, K.; Irie, H.; Sato, T.; Uchibori, A.; Shiozawa, M.; Tezuka, Y. *Macromolecules* **2005**, *38*, 10210.
(35) Hadjichristidis, N.; Pispas, S.; Pitsikalis, M. *Prog. Polym. Sci.* **1999**, *24*, 875.
(36) Binder, W. H.; Kunz, M. J.; Kluger, C.; Hayn, G.; Saf, R. *Macromolecules* **2004**, *37*, 1749.
(37) Tsarevsky, N. V.; Sumerlin, B. S.; Matyjaszewski, K. *Macromolecules* **2005**, *38*, 3558.
(38) Feldman, K. E.; Kade, M. J.; Meijer, E. W.; Hawker, C. J.; Kramer, E. J. *Macromolecules* **2009**, *42*, 9072.
(39) Zhang, H. Q.; Jiang, X. L.; Linde, R. V. D. *Polymer* **2004**, *45*, 1455.
(40) (a) Davidson, N. S.; Fetters, L. J.; Funk, W. G.; Graessley, W. W.; Hadjichristidis, N. *Macromolecules* **1988**, *21*, 112. (b) Fetters, L. J.; Graessley, W. W.; Hadjichristidis, N.; Kiss, A. D.; Pearson, D. S.; Younghouse, L. B. *Macromolecules* **1988**, *21*, 1644.
(41) Tanaka, F.; Edwards, S. F. *Macromolecules* **1992**, *25*, 1516.
(42) (a) Annable, T.; Buscall, R.; Ettelaie, R.; Wittelsetone, T. J. *J. Rheol.* **1993**, *37*, 695. (b) Ma, S. X.; Cooper, S. L. *Macromolecules* **2001**, *34*, 3294.
(43) (a) Antonietti, M.; Ehlich, D.; Foelsch, K. J.; Sillescu, H.; Schmidt, M.; Lindner, P. *Macromolecules* **1989**, *22*, 2802. (b) Antonietti, M.; Foelsch, K. J.; Sillescu, H.; Pakula, T. *Macromolecules* **1989**, *22*, 2812.
(44) Karatzas, A.; Talelli, M.; Vasilakopoulos, T.; Pitsikalis, M.; Hadjichristidis, N. *Macromolecules* **2006**, *39*, 8456.
(45) Karayianni, E.; Jerome, R.; Cooper, S. L. *Macromolecules* **1997**, *30*, 7444.
(46) Register, R. A.; Prud'homme, R. E. Melt Rheology. In *Ionomers: Synthesis, Structure, Properties, and Applications*; Tant, M. R., Mauritz, K. A.,Wilkes, G. L., Eds.; Blackie Academics & Professional: London, 1997.
(47) Vlassopoulos, D.; Pakula, T.; Fytas, G.; Pitsikalis, M.; Hadjichristidis, N. *J. Chem. Phys.* **1999**, *111*, 1760.
(48) Vlassopoulos, D.; Pitsikalis, M.; Hadjichristidis, N. *Macromolecules* **2000**, *33*, 9740.
(49) Pispas, S.; Hadjichristidis, N. *Macromolecules* **1994**, *27*, 1891.
(50) Storey, R. F.; George, S. E.; Nelson, M. E. *Macromolecules* **1991**, *24*, 2920.
(51) Pitsikalis, M.; Hadjichristidis, N.; Mays, J. W. *Macromolecules* **1996**, *29*, 179.
(52) Pitsikalis, M.; Hadjichristidis, N. *Macromolecules* **1995**, *28*, 3904.
(53) Charalambidis, D.; Pitsikalis, M.; Hadjichristidis, N. *Macromol. Chem. Phys.* **2002**, *203*, 2132.
(54) Young, R. N.; Quirk, R. P.; Fetters, L. J. *Adv. Polym. Sci.* **1984**, *56*, 1.
(55) (a) van Ruymbeke, E.; Kapnistos, M.; Vlassopoulos, D.; Huang, T. Z.; Knauss, D. M. *Macromolecules* **2007**, *40*, 1713. (b) van Ruymbeke, E.; Bailly, C.; Keunings, R.; Vlassopoulos, D. *Macromolecules* **2006**, *39*, 6248. (c) van Ruymbeke, E.; Orfanou, K.; Kapnistos, M.; Iatrou, H.; Pitsikalis, M.; Hadjichristidis, N.; Lohse, D. J.; Vlassopoulos, D. *Macromolecules* **2007**, *40*, 5941.
(56) van Ruymbeke, E.; Keunings, R.; Bailly, C. *J. Non-Newtonian Fluid Mech.* **2005**, *128*, 7.
(57) Marrucci, G. *J. Polym. Sci., Polym. Phys. Ed.* **1985**, *23*, 159.
(58) Ball, R. C.; McLeish, T. C. B. *Macromolecules* **1989**, *22*, 1911.
(59) Pakula, T.; Vlassopoulos, D.; Fytas, G.; Roovers, J. *Macromolecules* **1998**, *31*, 8931.
(60) Pusey, P. N. In *Liquids, Freezing, and Glass Transition*; Hansen, J. P., Levesque, D., Zinn-Justin, J., Eds.; NATO ASI; North Holland: Amsterdam, 1991.
(61) Hadjichristidis, N.; Pispas, S.; Floudas, G. *Block Copolymers*; Wiley: New York. 2002.
(62) Fetters, L. J.; Lohse, D. J.; Richter, D.; Witten, T. A.; Zirkel, A. *Macromolecules* **1994**, *27*, 4639.
(63) Liu, C. Y.; van Ruymbeke, E.; Keunings, R.; Bailly, C. *Polymer* **2006**, *47*, 4461.
(64) Weiss, R. A.; Zhao, H. Y. *J. Rheol.* **2009**, *53*, 191.
(65) Folmer, B. J. B.; Sijbesma, R. P.; Versteegen, R. M.; van der Rijt, J. A. J.; Meijer, E. W. *Adv. Mater.* **2000**, *12*, 874.
(66) Hirschberg, J. H. K. K.; Beijer, F. H.; van Aert, H. A.; Magusim, P.C. M. M.; Sijbesma, R. P.; Meijer, E. W. *Macromolecules* **1999**, *32*, 2696.
(67) Versteegen, R. M.; van Beek, D. J. M.; Sijbesma, R. P.; Vlassopoulos, D.; Fytas, G.; Meijer, E. W. *J. Am. Chem. Soc.* **2005**, *127*, 13862.
(68) Strobl, G. *The Physics of Polymers*, 2nd ed.; Springer: Berlin, 1997.
(69) Kow, T.; Hadjichristidis, N.; Morton, M.; Fetters, L. J. *Rubber Chem. Technol.* **1982**, *55*, 245.
(70) Vlassopoulos, D.; Fytas, G.; Pakula, T.; Roovers, J. *J. Phys.: Condens. Matter* **2001**, *13*, R855.
(71) Gotro, J. T.; Graessley, W. W. *Macromolecules* **1984**, *17*, 2767.
(72) Larson, R. G.; Sridhar, T.; Leal, L. G.; McKinley, G. H.; Likhtman, A. E.; McLeish, T. C. B. *J. Rheol.* **2003**, *47*, 809.
(73) *Standard Pressure-Volume-Temperature Data for Polymers*; Zoller, P., Walsh, D.; Eds.; Technomic Publishing Co.: New York, 1995.
(74) Liu, C. Y.; He, J. S.; Keunings, R.; Bailly, C. *Macromolecules* **2006**, *39*, 25.
(75) Cordier, P.; Tournilhac, F.; Soulie-Ziakovic, C.; Leibler, L. *Nature* **2008**, *451*, 977.
(76) Kapnistos, M.; Semenov, A. N.; Vlassopoulos, D.; Roovers, J. *J. Chem. Phys* **1999**, *111*, 1753.